

Afterglows as Diagnostics of Gamma Ray Burst Beaming

James E. Rhoads

*Kitt Peak National Observatory¹
950 N. Cherry Ave., Tucson, AZ 85719*

Abstract. If gamma ray bursts are highly collimated, radiating into only a small fraction of the sky, the energy requirements of each event may be reduced by several (up to 4–6) orders of magnitude, and the event rate increased correspondingly. The large Lorentz factors ($\Gamma \gtrsim 100$) inferred from GRB spectra imply relativistic beaming of the gamma rays into an angle $\sim 1/\Gamma$. We are at present ignorant of whether there are ejecta outside this narrow cone.

Afterglows allow empirical tests of whether GRBs are well-collimated jets or spherical fireballs. The bulk Lorentz factor decreases and radiation is beamed into an ever increasing solid angle as the burst remnant expands. It follows that if gamma ray bursts are highly collimated, many more optical and radio transients should be observed without associated gamma rays than with them. In addition, a burst whose ejecta are beamed into angle ζ_m undergoes a qualitative change in evolution when $\Gamma\zeta_m \lesssim 1$: Before this, $\Gamma \propto r^{-3/2}$, while afterwards, $\Gamma \propto \exp(-r/r_r)$. This change results in a potentially observable break in the afterglow light curve.

Successful application of either test would eliminate the largest remaining uncertainty in the energy requirements and space density of gamma ray bursters.

The ejecta from gamma ray bursts must be highly relativistic to explain the spectral properties of the emergent radiation [1,4]. The gamma rays we observe are therefore only those from material moving within angle $1/\Gamma$ of the line of sight, and offer no straightforward way of determining whether the bursts are isotropic emitters or are beamed into a small angle. (Here Γ is the bulk Lorentz factor of expansion.)

Afterglow emission at longer wavelengths is expected to arise later in the evolution of the burst than the original gamma rays. It therefore offers at least two ways of testing the burst beaming hypothesis.

¹⁾ Kitt Peak National Observatory is part of the National Optical Astronomy Observatories, operated by the Association of Universities for Research in Astronomy.

Burst and Afterglow Event Rates

First, because Γ is lower at the time of afterglow emission than during the GRB itself, the afterglow cannot be as collimated as the GRB can. This implies that the afterglow event rate should exceed the GRB event rate substantially if bursts are strongly beamed. Allowing for finite detection thresholds,

$$\frac{N_{12}}{N_2} \leq \frac{\Omega_1}{\Omega_2} \leq \frac{N_1}{N_{12}} \quad , \quad (1)$$

where N_1 , N_2 are the measured event rates above our detection thresholds at our two frequencies; N_{12} is the rate of events above threshold at both frequencies; and Ω_1 , Ω_2 are the solid angles into which emission is beamed at the two frequencies.

A full derivation of this result and discussion of its application is given in [6]. Rather than reproduce it, I will refer the reader to that paper and will here discuss the second test more fully than was possible in [6].

Dynamical Calculations: Numerical Integrations

The second test is based on differences between the dynamical evolution of beamed and isotropic bursts. We explore the effects of beaming on burst evolution using the notation of [5]. Let Γ_0 and M_0 be the initial Lorentz factor and ejecta mass, and ζ_m the opening angle into which the ejecta move. The burst energy is $E = \Gamma_0 M_0 c^2 \zeta_m^2 / 4$, where we assume a unipolar jet geometry. Let r be the radial coordinate in the burster frame; t , t_{co} , and t_{\oplus} the time from the event measured in the burster frame, comoving ejecta frame, and terrestrial observer's frame; and f the ratio of swept up mass to M_0 .

The key assumptions in our beamed burst model are that (1) the energy and mass per unit solid angle are constant at angles $\theta < \zeta_m$ from the jet axis and zero for $\theta > \zeta_m$ (see [2] for an alternative model); (2) the energy in the ejecta is approximately conserved; (3) the ambient medium has uniform density; and (4) the cloud of ejecta + swept-up material expands in its comoving frame at the sound speed $c_s = c/\sqrt{3}$ appropriate for relativistic matter. The last of these assumptions implies that the working surface of the expanding remnant has a transverse size $\sim \zeta_m r + c_s t_{co}$. The evolution of the burst changes when the second term dominates over the first.

The full equations describing the burst remnant's evolution are then

$$f = \frac{1}{M_0} \int_0^r r^2 \Omega_m(r) \rho(r) dr \quad , \quad (2)$$

$$\Omega_m = \pi(\zeta_m + c_s t_{co}/ct)^2 \approx \pi(\zeta_m + t_{co}/\sqrt{3}t)^2 \quad , \quad (3)$$

$$\Gamma = (\Gamma_0 + f) / \sqrt{1 + 2\Gamma_0 f + f^2} \approx \sqrt{\Gamma_0/2f} \quad , \quad (4)$$

$$t = r/c \quad , \quad t_{co} = \int_0^t dt' / \Gamma \quad , \quad \text{and} \quad t_{\oplus} = \int_0^t dt' / 2\Gamma^2 \quad . \quad (5)$$

These equations can be solved by numerical integration to yield $f(r)$, $\Gamma(r)$, and $t_{\oplus}(r)$. Figure 1 shows $\Gamma(r)$ from such integrations for an illustrative pair of models (one beamed, one isotropic).

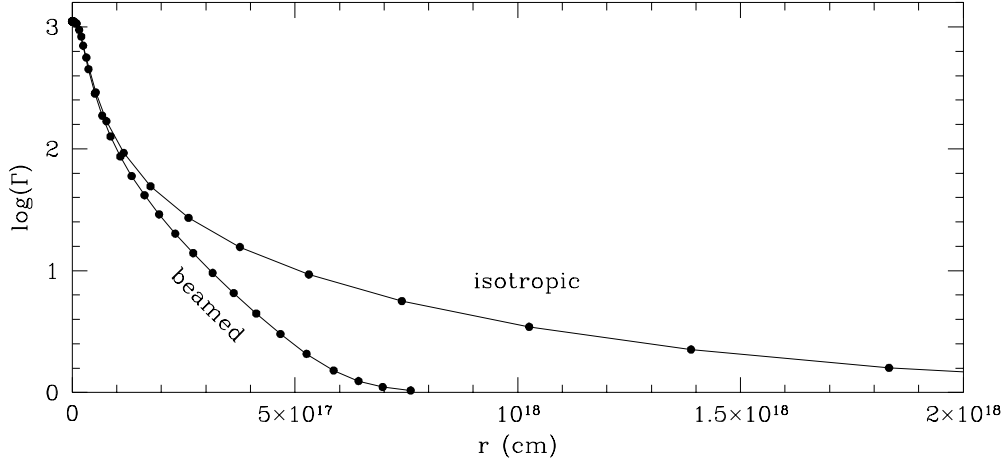


FIGURE 1. Dependence of the bulk Lorentz factor Γ on the burst expansion radius for an isotropic burst and a burst beamed into an opening angle $\zeta_m = 0.01$ radian. Both bursts follow a $\Gamma \propto r^{-3/2}$ evolution initially, but the beamed burst changes its behavior at $\Gamma \approx 100 \approx 1/\zeta_m$, beyond which its Lorentz factor decays exponentially with radius.

The emergent synchrotron radiation can also be calculated if we assume an electron energy spectrum and assume that electrons and magnetic fields have constant fractions of the equipartition energy density. For illustrative purposes, we again follow the assumptions in [5]. The electron energy spectrum is $N(\mathcal{E}) \propto \mathcal{E}^{-2}$, i.e. a power law with equal energy per decade, so that the synchrotron spectrum peaks where $\tau = 0.35$, rising as $\nu^{5/2}$ at low (optically thick) frequencies and falling as $\nu^{-1/2}$ at high (optically thin) frequencies [3]. The relevant equations are a straightforward modification of equations 11–20 of [5]. Figure 2 shows the peak flux density as a function of observed frequency for the models used in figure 1. We caution the reader that more recent electron energy spectra grounded in observations (e.g. [7]) may be more reliable. We hope to incorporate such spectra in our calculations in future.

Dynamical Calculations: Analytic Integrations

The most interesting dynamical change introduced by beaming is a transition from a power law $\Gamma \propto r^{-3/2}$ to an exponentially decaying regime $\Gamma \propto \exp(-r/r_r)$. This can be derived by considering the approximate evolution equations for the

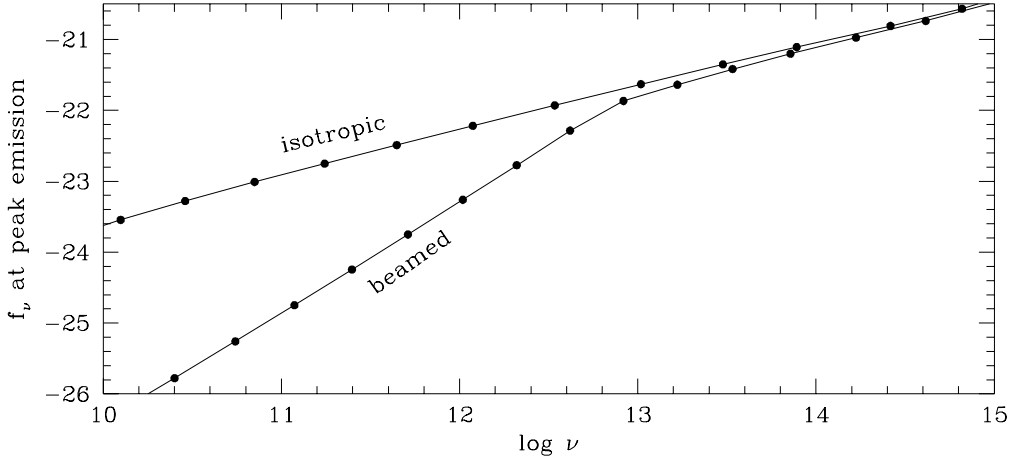


FIGURE 2. The dependence of the peak flux density f_ν on observed frequency ν for the same pair of bursts. The electron spectrum follows the model of Paczyński & Rhoads (1993). The peak in the synchrotron emission for this model occurs at the frequency where optical depth effects become important. The predicted break in the power law caused by beaming should be observable. Similar breaks occur in the dependence of f_ν and ν_{peak} with time, and are expected to be a generic feature of beamed GRB afterglow models.

regime where (a) $1/\Gamma_0 \lesssim f \lesssim \Gamma_0$, so that $\Gamma \approx \sqrt{\Gamma_0/2f}$; and (b) $c_s t_{co} > \zeta_m r$ (corresponding to $f \gtrsim 9\Gamma_0 \zeta_m^2$):

$$df/dr \approx \frac{\pi}{M_0} c_s^2 t_{co}^2 \rho \quad , \quad dt_{co}/dr \approx \sqrt{\frac{2f}{c^2 \Gamma_0}} \quad , \quad dt_\oplus/dr \approx \frac{f}{c \Gamma_0} \quad . \quad (6)$$

It follows that

$$\sqrt{f} df = \frac{\pi}{\sqrt{2}} \frac{c c_s^2 \rho \sqrt{\Gamma_0}}{M_0} \times t_{co}^2 dt_{co} \approx \frac{\pi}{3\sqrt{2}} \frac{c^3 \rho \sqrt{\Gamma_0}}{M_0} \times t_{co}^2 dt_{co} \quad . \quad (7)$$

This is easily integrated to obtain

$$f^{3/2} = \left(\frac{\pi \sqrt{\Gamma_0} c c_s^2 \rho}{\sqrt{8} M_0} \right) t_{co}^3 + const \quad . \quad (8)$$

The constant of integration becomes negligible once $c_s t_{co} \gg \zeta_m r$, so that equation 8 becomes $f \propto t_{co}^2$. It is then clear from equations 6 that f , Γ , t_{co} , and t_\oplus will all behave exponentially with r in this regime. Retaining the constants of proportionality, we find

$$f \propto \exp(2r/r_\Gamma) \quad \text{where} \quad r_\Gamma = \left[\frac{1}{\pi} \left(\frac{c}{c_s} \right)^2 \frac{\Gamma_0 M_0}{\rho} \right]^{1/3} \quad . \quad (9)$$

Further algebra yields $\Gamma \propto \exp(-r/r_r)$ and $t_{\oplus} \propto f \propto \exp(2r/r_r)$, so that $\Gamma \propto t_{\oplus}^{-1/2}$. Thus, while the evolution of $\Gamma(r)$ changes from a power law to an exponential at $\Gamma \sim 1/\zeta_m$, the evolution of $t_{\oplus}(r)$ changes similarly. The net result is that $\Gamma(t_{\oplus})$ has a power law form in both regimes, but with a break in the slope from $\Gamma \propto t_{\oplus}^{-3/8}$ when $\Gamma > 1/\zeta_m$ to $\Gamma \propto t_{\oplus}^{-1/2}$ when $\Gamma < 1/\zeta_m$.

Of course, Γ is not directly observable, and we ultimately want to predict observables like the frequency of peak emission ν_m , the flux density $F_{\nu,m}$ at ν_m , and the angular size θ of the afterglow. With the electron energy spectrum described above, the relevant power law scalings before beaming becomes dynamically important are $\nu_m \sim t_{\oplus}^{-2/3}$, $F_{\nu,m} \sim t_{\oplus}^{-5/12}$, and $\theta \sim t_{\oplus}^{5/8}$. At late times, $\nu_m \sim t_{\oplus}^{-1}$, $F_{\nu,m} \sim t_{\oplus}^{-3/2}$, and $\theta \sim t_{\oplus}^{1/2}$. Our numerical integrations confirm these relations, though the transition between the two regimes is quite gradual for ν_m .

Combining these scalings with the spectral shape yields predictions for the light curve at fixed observed frequency. The most dramatic feature is in the light curve shape for $\nu > \nu_m$, which changes from $F_{\nu,\oplus} \sim t_{\oplus}^{-3/4}$ to $F_{\nu,\oplus} \sim t_{\oplus}^{-2}$. These exponents are generally sensitive to the assumed electron energy distribution in the blast wave.

Conclusions

Establishing whether or not gamma ray bursts are beamed will be valuable in understanding source populations and burst mechanisms. There are at least two potentially observable consequences of beaming.

(1) The event rate for afterglows should exceed that for bursts substantially if bursts are strongly beamed. A quantitative comparison of rates at two frequencies yields quantitative limits on the ratio of beaming angles.

(2) The dynamical evolution of a beamed burst remnant changes qualitatively when $\Gamma < 1/\zeta_m$. The resulting changes in the light curves could be observed.

REFERENCES

1. Goodman, J. 1986, *ApJ* 308, L47
2. Mészáros, P., Rees, M. J., & Wijers, R. A. M. J. 1997, astro-ph/9709273
3. Pacholczyk, A. G. 1970, *Radio Astrophysics*, San Francisco: W. H. Freeman
4. Paczyński, B. 1986, *ApJ* 308, L43
5. Paczyński, B., & Rhoads, J. E. 1993, *ApJ* 418, L5
6. Rhoads, J. E. 1997, *ApJ* 487, L1
7. Waxman, E. 1997, *ApJ* 485, L5